Proceedings of the 10th International Conference on Energy Sustainability
ES2016
June 26 – June 30, 2016, Charlotte, North Carolina, USA

PowerEnergy2016-59463

Calorimetric Evaluation of Novel Concentrating Solar Receiver Geometries with Enhanced Effective Solar Absorptance

Jesus D. Ortega
Sandia National Laboratories, Concentrating Solar Technologies Department
Albuquerque, NM 87185-1127, USA.

Julius E. Yellowhair
Sandia National Laboratories, Concentrating Solar Technologies Department
Albuquerque, NM 87185-1127, USA.

Clifford K. Ho
Sandia National Laboratories, Concentrating Solar Technologies Department
Albuquerque, NM 87185-1127, USA.

Joshua M. Christian
Sandia National Laboratories, Concentrating Solar Technologies Department
Albuquerque, NM 87185-1127, USA.

Charles E. Andraka
Sandia National Laboratories, Concentrating Solar Technologies Department
Albuquerque, NM 87185-1127, USA.

ABSTRACT

Direct solar power receivers consist of tubular arrays, or panels, which are typically tubes arranged side by side and connected to an inlet and outlet manifold. The tubes absorb the heat incident on the surface and transfer it to the fluid contained inside them. To increase the solar absorptance, high temperature black paint or a solar selective coating is applied to the surface of the tubes. However, current solar selective coatings degrade over the lifetime of the receiver and must be reapplied, which reduces the receiver thermal efficiency and increases the maintenance costs. This work presents an evaluation of several novel receiver shapes which have been denominated as fractal like geometries (FLGs). The FLGs are geometries that create a light-trapping effect, thus, increasing the effective solar absorptance and potentially increasing the thermal efficiency of the receiver. Five FLG prototypes were fabricated out of Inconel 718 and tested in Sandia's solar furnace at two irradiance levels of ~15 and 30 W/cm^2 and two fluid flow rates. Photographic methods were used to capture the irradiance distribution on the receiver surfaces and compared to results from ray-tracing models. This methods provided the irradiance distribution and the thermal input on the FLGs. Air at nearly atmospheric pressure was used as heat transfer fluid. The air inlet and outlet temperatures were recorded, using a data acquisition system, until steady state was achieved. Computational fluid dynamics (CFD) models, using the Discrete Ordinates (DO) radiation and the k-ω Shear Stress Transport (SST) equations, were developed and calibrated, using the test data, to predict the performance of the five FLGs at different air flow rates and irradiance levels. The results showed that relative to a flat plate (base case), the new FLGs exhibited an increase in the effective solar absorptance from 0.86 to 0.92 for an intrinsic material absorptance of 0.86. Peak surface temperatures of ~1000^{o}C and maximum air temperature increases of ~200^{o}C were observed. Compared to the base case, the new FLGs showed a clear air outlet temperature increase. Thermal efficiency increases of ~15%, with respect to the base case, were observed. Several tests, in different days, were performed to assess the repeatability of the results. The results obtained, so far, are very encouraging and display a very strong potential for incorporation in future solar power receivers.

1. INTRODUCTION

External direct receivers are typical for CSP technologies and have been the focus of many studies and experiments. Solar One and Solar Two (Figure 1) receivers were composed of many tubes which form panels which in turn are arranged in a cylindrical configuration. The Solar Two receiver showed a thermal efficiency of up to 88% [1], but not continuously. The current SunShot initiative requires a thermal efficiency of greater than 90% [2] which has never been designed before. New advances in receiver design must be completed in order to achieve this performance requirement. One way is by manipulating the receiver geometry or adding special features,

the view factors can be altered and the thermal efficiency could be increased by reducing radiative heat loss from the system. A report by Garbrecht et al. showed that the use of pyramidal structures could reduce reflective loses by 1.3% [3]. Nonetheless, the main disadvantage of the pyramid structures are the hot spots created at the peaks of the structures due to stagnant flow conditions. Rocketdyne reported an initial evaluation in some star receiver geometry concepts in 1974 [4]. However, the thermal efficiency advantages of the receivers were not fully evaluated due to the complexity of the problem, at the time. Sandia National Laboratories (SNL) has invented [5] several "light-trapping" geometries which take advantage of reduced view factors which could increase thermal efficiency of external direct receivers.

Figure 1. Left: Solar One receiver panel. Right: Solar Two receiver panel.

Previously, ray-tracing models and experiments were conducted by Yellowhair et al. [6] intended to demonstrate a potential increase in solar absorptivity by creating a light trapping effect in several types of geometries (Figure 2) by using patterns which could create multiple reflections. The on-sun tests of these fractal-like geometries (FLGs) were performed using the solar furnaces at the SNL National Solar Thermal Test Facility (NSTTF). In the other hand, SolTrace [7] was used to develop a computational model of the solar furnace to show an increase in the effective solar absorptance in the FLGs.

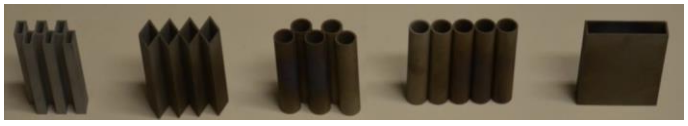

Figure 2. Prototype FLGs fabricated with additive manufacturing using Inconel 718 [5].

The results presented by Yellowhair et al. (Figure 3) showed that for the FLGs, there can be multiple reflections between the surfaces causing a light-trapping effect. This leads to a higher solar absorptivity. Relative to a flat plate, FLGs increase the effective solar absorptance from 0.86 to 0.915 for an intrinsic material absorptance of 0.86 (i.e. oxidized Inconel 718).

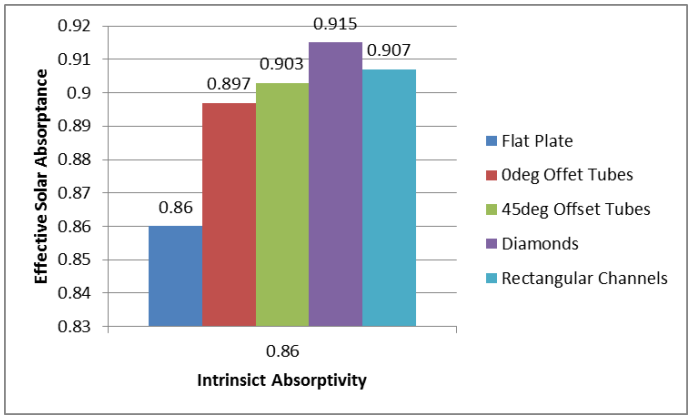

Figure 3. Results of the ray-tracing simulations showing absorptance improvements from the fractal-like geometries relative to a flat plate receiver.

Nevertheless, the increase in effective solar absorptance does not correlate with a potential increase in thermal efficiency. The overarching goal of this work is to evaluate the thermal efficiency of the FLGs and study the potential implementation in full-scale direct receivers.

2. APPROACH

In order to evaluate the thermal efficiency of the FLGs, two manifolds were added to the geometries which are connected to a test rig. The manifolds consist of a rectangular channels that are attached at the bottom and top of the part with inlet and outlet ports, respectively. These ports can be connected to the test rig by using a Swagelok fitting. These new parts were built out of Inconel 718 metal using the direct metal laser sintering (Figure 4). The samples were oxidized for 20 hours at 800^{o}C in order to achieve the solar absorptivity

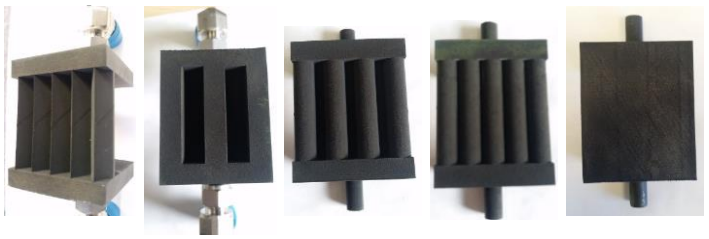

Figure 4. New FLGs with manifolds manufactured by Sigma Labs (Santa Fe, NM). From left to right: diamond channels, rectangular channels, 45° offset cylinder tubes, 0° offset cylinder tubes, and flat plate [5].

These FLGs have a frontal area of ~5 cm x 5 cm which matches the beam size from the solar furnace. The parts were built with a

wall thickness of 1 mm to minimize the amount of material required for construction. The test loop is a calorimetric setup built to evaluate the thermal performance of the receivers. The complete test loop was composed by an air blower, a regulating valve, an air flow meter, and a thermocouple in the inlet and the outlet (Figure 5). The test loop was able to accommodate all the FLGs to be tested in the solar furnace.

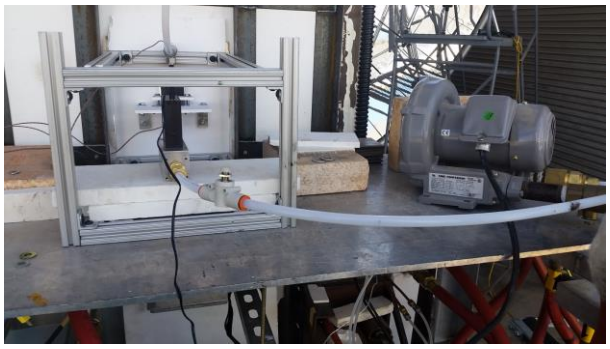

Figure 5. Complete test loop.

Spillage board was required to avoid flux spillage to the rest of the test loop components (Figures 6 and 7). This also limited the irradiance that will intersect other regions of the part.

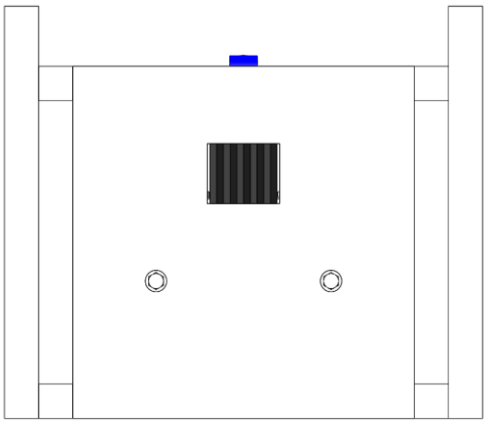

Figure 6. Spillage board located in the front of FLG mount. Aperture dimensions (W x L): 5 cm x 5.1 cm.

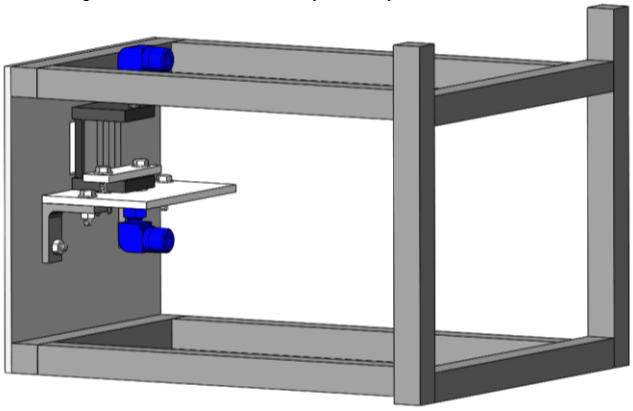

Figure 7. FLG complete mount. The part is located ~1.5 mm behind the 6.35 mm spillage board.

2.1. Solar Furnace Testing

The solar furnace at the SNL National Solar Thermal Test Facility (NSTTF) is capable of providing 16 kW thermal power and up to 7000 W/cm^2 peak irradiance over a 5 cm beam size [6]. The FLGs were placed at the focus of the dish concentrator while the blower was running at 50 SLPM (i.e. Standard liters per minute). The attenuator was then opened enough to reach two concentration levels ~15 and 30 W/cm^2. The concentration levels were measured using a flux Kendall. The attenuator settings were in turn used to apply a heat flux on the FLGs. Inlet and outlet temperatures were recorded along with the flow rate and direct normal irradiance (DNI). Photographs were taken during the tests and were analyzed with the PHLUX tool [8] as shown in Figure 8a and 8b.

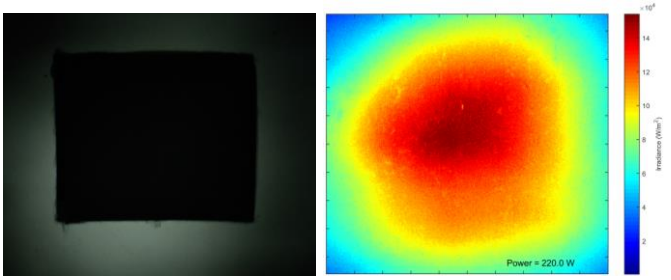

Figure 8a. Left: Heat flux incident on the flat plate. Right: Heat flux applied on the FLGs ~15 W/cm^2.

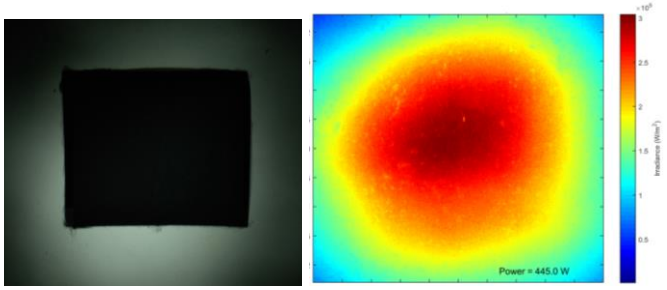

Figure 8b. Left: Heat flux incident on the flat plate. Right: Heat flux applied on the FLGs ~30 W/cm^2.

The heat fluxes in Figure 8a and 8b represent the heat flux distribution on a flat surface. The heat flux incident on this surface is the same used on the part. This heat flux is applied using the geometric center of the part as the aim-point.

After the tests were completed, the flow rate was reduced to ~35 SLPM and the outlet temperatures were targeted to match to those in the previous tests. The attenuator setting were adjusted in order to achieve equal outlet temperatures. These high and low equivalent fluxes varied between FLGs and they are presented in table 1.

The peak surface temperatures were monitored using a laser thermometer. The peak surface temperature was used as a separate measure to build the computational models. Peak temperatures of ~1000°C were recorded due to the limited flow rates that the blower was able to provide.

Table 1 shows the incident heat calculated for every case. The results (Figure 9) show an increase in the thermal efficiency when compared to the flat plate in all instances. The increase in thermal efficiency can be attributed to the light-trapping and by the features of the FLGs.

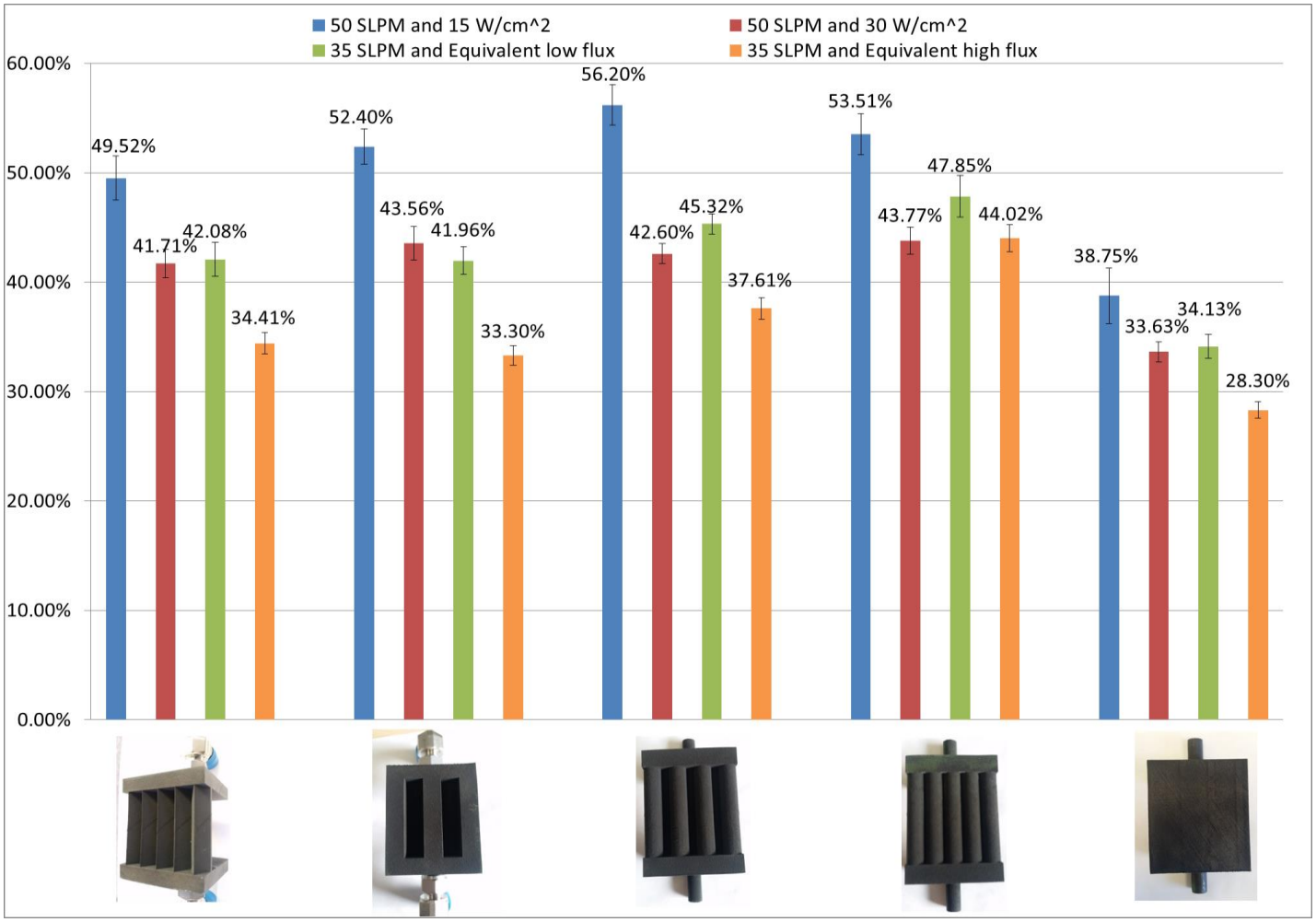

Figure 9. Thermal efficiency of FLGs. The equivalent high and low fluxes were estimated to match the outlet temperature of the 30 W/cm^2 and 15 W/cm^2 tests, respectively.

2.2 THERMAL EFFICIENCY RESULTS

The thermal efficiency is evaluated as shown in equation 1. Where $\dot{Q}_{abs}$ is the heat is absorbed by the air flow and $\dot{Q}_{in}$ is the heat incident on the part. The values of the heat incident on the part are based on the amount of heal flux that intersects the aperture over the size of the aperture.

$$\eta = \frac{\dot{Q}_{abs}}{\dot{Q}_{in}} \qquad (1)$$

Table 1. The Incident power applied to the FLGs.

	Flux Level (W/cm^2)	Power on Aperture (W)	Flux Level (W/cm^2)	Power on Aperture (W)
Diamond	15	229	13	184
	30	462	26	392
Rectangular	15	213	11	167
	30	438	25	377
45° offset	15	221	13	194
	30	445	27	381
0° offset	15	220	11	156
	30	444	21	300
Flat Plate	15	214	13	162
	30	439	28	359

Table 1 contains the incident power on the apertures which corresponds to the specified flux level. The values on the left correspond to the two flux levels on every part while air was flowing at 50 SLPM. The values on the right correspond to the equivalent low and high flux levels which yield similar outlet temperature at a 35 SLPM air flow rate.

The absorbed heat was calculated as:

$$\dot{Q_{abs}} = \dot{m} \int_{T_{in}}^{T_{out}} C_p dT \qquad (2)$$

Where $\dot{m}$ is the mass flow rate measured, Cp is the heat capacity of air as function of temperature and T_{in} and T_{out} are the measured inlet and outlet temperatures. Since there are small fluctuations in the measurements, the propagated error throughout our measurements was computed by means of the root sum squared (RSS) using equation 3.

$$\sigma_{sys} = \sqrt{\left(\sum_{i=1}^{n} \frac{\sigma_i}{\mu_i}\right)^2}$$

Where σ_{sys} is the equivalent standard deviation of the measurements, n is the number of variables, σ_i is the standard deviation of the individual variables and μ_i is the mean of the individual variable measurements. The RSS provides a general standard deviation for all the measurements combined.

3. COMPUTATIONAL MODELING

Computational simulations were performed using ANSYS Fluent were developed using the test results to tune the parameters specified. These models provide a flexibility to analyze in detail the flow dynamics and the heat transfer across the FLGs. The goal of these models is to be able to predict the thermal efficiencies in the future by using the test results to fine-tune the models.

3.1. Fluid Dynamics

The k-ω Shear Stress Transport (SST) model was used to solve for the turbulent flow inside the FLGs. This model can accommodate a mesh with larger near-wall cells by handling Y+ values from 30 to 300. Initially the flow and turbulence equations were solved before the energy and radiation equations were enabled. Figure 10 shows the velocity contours of the air flow in different positions throughout the part.

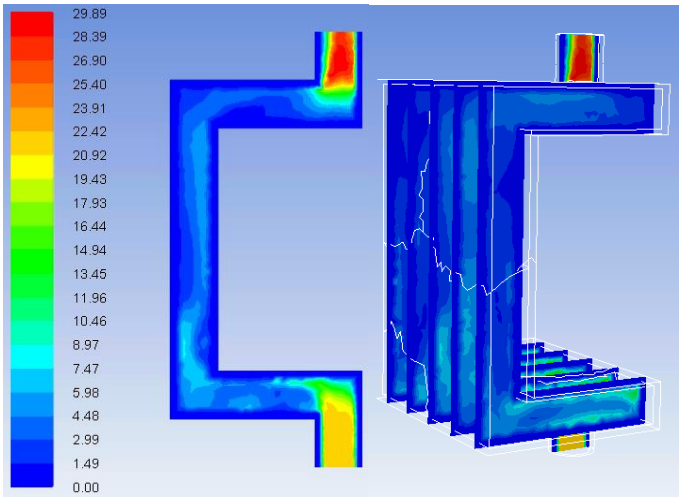

Figure 10. Velocity contours of the air flow across the Flat Plate. Left: Central cross-sectional plane. Right: Five cross-sectional planes with one centimeter separation.

3.2. Radiative and Convective Heat Transfer

The discrete ordinates (D. O.) radiation model was used to solve the conjugate heat transfer throughout the FLGs. Air is assumed to be a participating medium with an absorption coefficient of 0. Oxidized Inconel 718 has a measured emittance of 0.8 and a single band (i.e. infrared) is assumed.

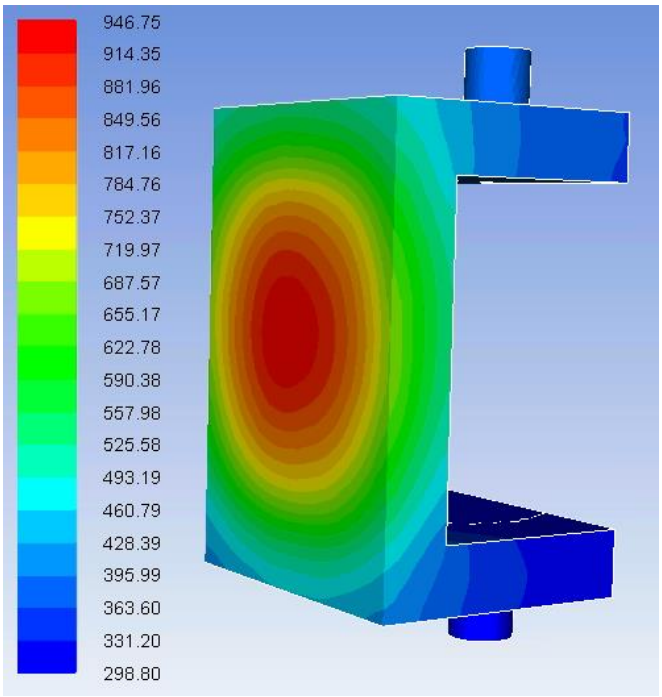

Figure 11a. Temperature contour of the Flat Plate surface with an incident flux of 15 W/cm^2.

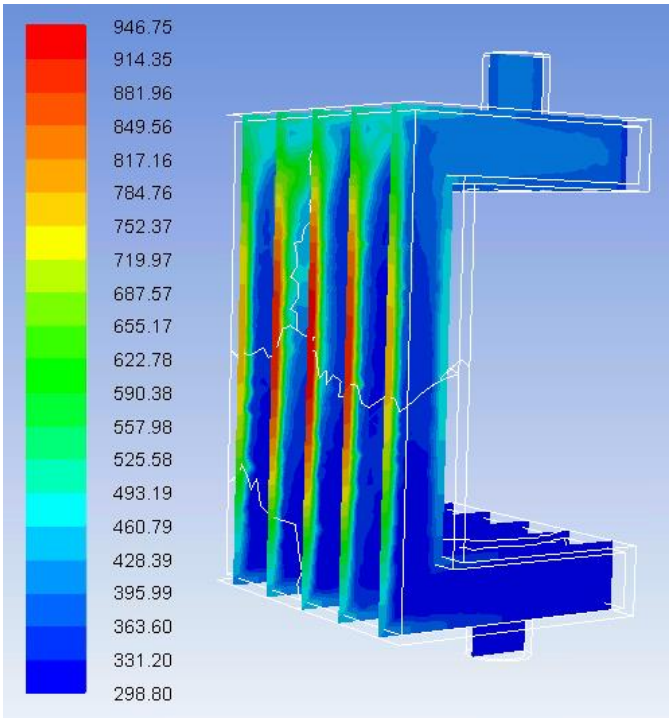

Figure 11b. Temperature contours of the air flow across the Flat Plate with an incident flux of 15 W/cm^2. Five cross-sectional planes with one centimeter separation.

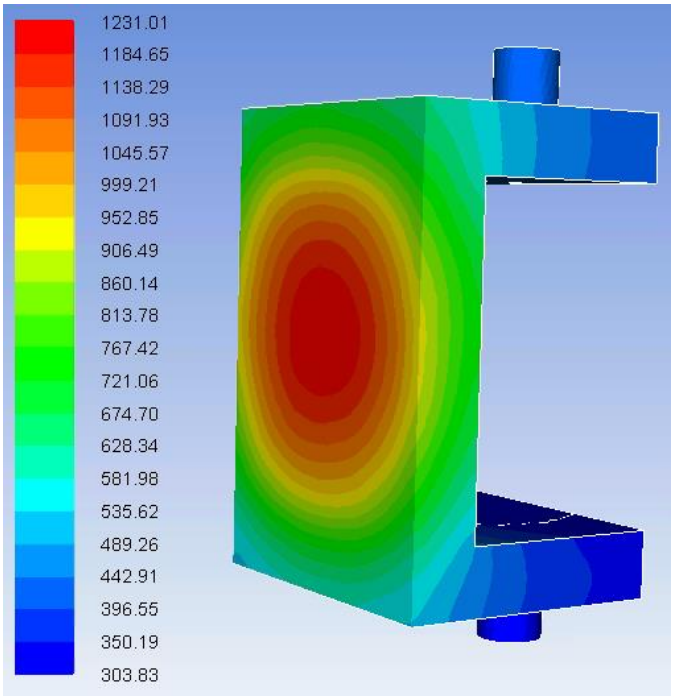

Figure 12a. Temperature contour of the Flat Plate surface with an incident flux of 30 W/cm^2.

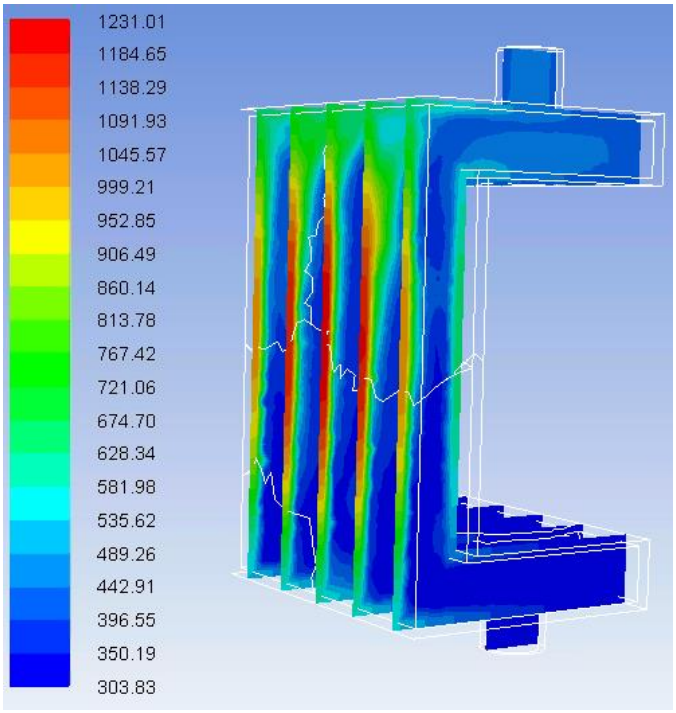

Figure 12b. Temperature contours of the air flow across the Flat Plate with an incident flux of 30 W/cm^2. Five cross-sectional planes with one centimeter separation.

Figures 11a - 12b show the temperature contours on the surface and in specific regions of the fluid zone inside the part. These temperatures are compared to the measured temperatures in the tests. Figures 13 and 14 show the comparison between temperatures measured and temperatures modeled.

In both figures, the temperatures correspond to the first 2 cases (i.e. 15 and 30 W/cm^2) and 50 SLPM air flow rate, respectively.

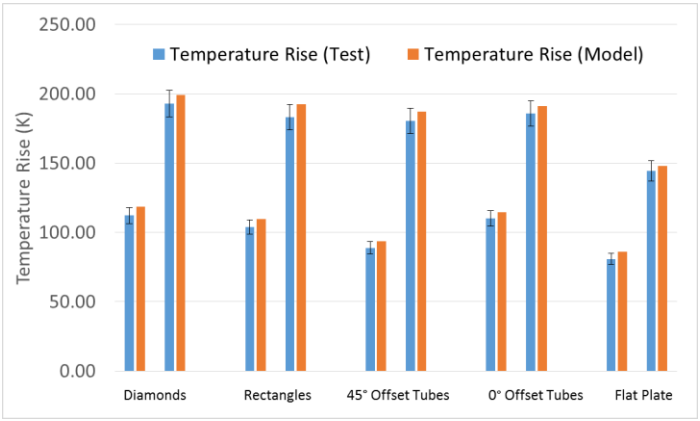

Figure 13. Measured and simulated air-temperature rise during tests of FLGs. Error bars represent the standard deviation on the measurements.

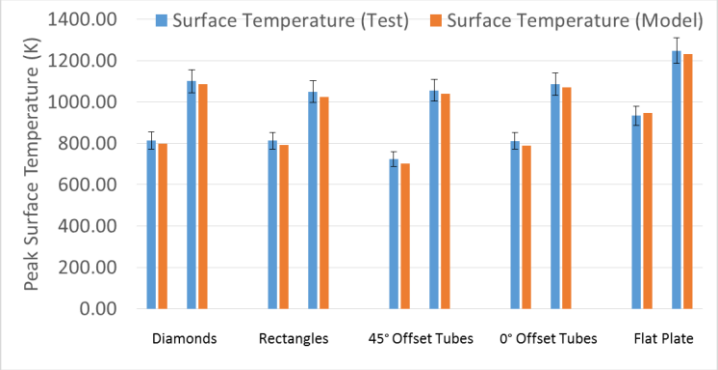

Figure 14. Measured and simulated peak surface temperatures during tests of FLGs. Error bars represent the standard deviation on the measurements.

The temperatures obtained from the models were found to be comparable to the ones measured in the tests. There are several reasons why the temperatures don't match exactly. First, there are some variations that occur from the wind in different days. This directly relates to the convective losses. Also, the heat transferred to the components in contact with the FLGs (i.e. connectors and mount), which was not accounted for in the models.

4. CONCLUSIONS

The efficiencies of the FLGs were higher than the flat plate and this increase can be attributed to the light-trapping features. This effect could be potentially greater if a heat transfer fluid with better thermal properties was used. Nonetheless, structural and design optimization analyses need to be performed in order to ensure the durability and while maintaining the best performance of the receiver.

For the set flow rates, 35 and 50 SLPM, the parts perform best at the lower heat flux levels. This is due to the high surface temperatures (Figure 14) which are resulting from air's limitation as heat transfer fluid and the limitations on the maximum flow rate that the blower could provide.

In the case where the outlet temperature was prescribed, the runs with the higher flux level and higher flow rates yielded higher efficiencies when compared to those with lower heat flux level and lower flow rates. This is expected simply by energy balance. A higher flow rate will yield larger heat transfer to the fluid, yielding higher thermal efficiency.

The computational models developed were very useful to understand the behaviour of the heat transfer across the FLGs. As it was observed, there were some differences on the temperature rise of the air and peak surface temperature in the models and in the tests. These variations can be attributed to the variability of wind in different days, which increases the convective losses, and the heat transferred to the components in contact with the FLGs, which was not accounted for in the models.

Although the thermal efficiency of the FLGs relative to the baseline case (i.e. flat plate) indeed increased, the conventional tubes performed the best. This is attributed to an increase in surface area by the other parts. Although the temperature rise and surface temperatures of all FLGs was very close, a clear difference was observed compared to the baseline case.

5. AKNOWLEDGMENTS

Sandia National Laboratories is a multi-program laboratory managed and operated by Sandia Corporation, a wholly owned subsidiary of Lockheed Martin Corporation, for the U.S. Department of Energy's National Nuclear Security Administration under contract DE-AC04-94AL85000. The United States Government retains and the publisher, by accepting the article for publication, acknowledges that the United States Government retains a non-exclusive, paid-up, irrevocable, world-wide license to publish or reproduce the published form of this manuscript, or allow others to do so, for United States Government purposes.

6. REFERENCES

[1] Pacheco, J. E., 2002, "Final Test and Evaluation Results from the Solar Two Project," SAND2002-0120, Sandia National Laboratories.

[2] U. S. Department of Energy,., 2011, "SunShot Initiative."

[3] Garbrecht, O., Al-Sibai, F., Kneer, R., and Wieghardt, K., 2013, "CFD-simulation of a new receiver design for a molten salt solar power tower," Solar Energy(90), pp. 94-106.

[4] Friefield, J. M., and Friedman, J., 1974, "Technical Report No. 1: Solar Thermal Power Systems Baded on Optical Transmission,"Rocketdyne Division, Rockwell International.

[5] Ho, C., Christian, J., Pye, J., Ortega, J., "U.S. Patent Application 14535100, Filed Nov. 6, 2014, BLADED SOLAR THERMAL RECEIVERS FOR CONCENTRATING SOLAR POWER."

[6] Yellowhair, J., Ho, C., Ortega, J., Andraka, C., 2015, "Testing and Optical Modeling of Novel Concentrating Solar Receiver Geometries to Increase Light Trapping and Effective Solar Absorptance", SPIE 2015 SPIE Optics + Photonics Conference San Diego, CA.

[7] National Renewable Energy Laboratory, "SolTrace Optical Modeling Software", Golden, CO, http://www.nrel.gov/csp/soltrace/.

[8] C. K. Ho, and S. S. Khalsa, "A Photographic Flux Mapping Method for Concentrating Solar Collectors and Receivers," Journal of Solar Energy Engineering-Transactions of the ASME, 134(4), (2012).